Plasmon-polariton waves in nanofilms on one-dimensional photonic crystal surfaces

2010 New J. Phys. 12 093006

(http://iopscience.iop.org/1367-2630/12/9/093006)

New Journal of Physics
The open-access journal for physics

Plasmon-polariton waves in nanofilms on one-dimensional photonic crystal surfaces

Valery N Konopsky
Institute of Spectroscopy, Russian Academy of Sciences, Fizicheskaya 5, Troitsk, Moscow Region 142190, Russia
E-mail: konopsky@gmail.com

New Journal of Physics **12** (2010) 093006 (18pp)
Received 20 May 2010
Published 6 September 2010
Online at http://www.njp.org/
doi:10.1088/1367-2630/12/9/093006

Abstract. The propagation of bound optical waves along the surface of a one-dimensional (1D) photonic crystal (PC) structure is considered. A unified description of the waves in 1D PCs for both s- and p-polarizations is done via an impedance approach. A general dispersion relation that is valid for optical surface waves with both polarizations is obtained, and conditions are presented for long-range propagation of plasmon-polariton waves in nanofilms (including lossy ones) deposited on the top of the 1D PC structure. A method is described for designing 1D PC structures to fulfill the conditions required for the existence of the surface mode with a particular wavevector at a particular wavelength. It is shown that the propagation length of the long-range surface plasmon polaritons in a thin metal film can be maximized by wavelength tuning, which introduces a slight asymmetry in the system.

Contents

1. Introduction **2**
2. Dispersion relation for s- and p-polarized surface waves in impedance terms **4**
2.1. Impedance approach: basic definitions and the recursion relation for a multilayer 4
2.2. The input impedance of a semi-infinite one-dimensional photonic crystal (1D PC) 6
2.3. Dispersion relation for SWs 7
2.4. Band gap maximum extinction per length 8
3. Calculation of the 1D PC structure for particular experimental conditions **8**
3.1. Angle-dependent variables 8
3.2. Conditions for long-range propagation of the plasmon-polariton waves in metal films 9
3.3. Derivation of d_1, d_2 and d_3 for the PC structure terminated by a Pd nanofilm . . 11
4. Conclusions **13**
Acknowledgments **13**
Appendix A. Dispersion relation for long-range surface plasmon polaritons (LRSPPs) in the symmetrical configuration and the increase of propagation length associated with slight asymmetry in the system **13**
Appendix B. Additional damping in a thin film **16**
References **18**

1. Introduction

Optical surface waves (SWs) are excitations of electromagnetic (EM) modes that are bound to the interface between two media. The maximum EM field strength of the SWs is located near the interface, so these waves have a high sensitivity to the surface condition. The SWs that have been employed in the widest array of applications are surface plasmon-polariton (SPP) waves, which are p-polarized optical SWs propagated along a metal–dielectric interface [1]. The sensitivity of SPPs has been used in many surface plasmon resonance (SPR) applications in which a shift of an SPR dip is measured, from biosensors used for detecting biomolecules in a liquid to gas sensors for detecting trace impurities in the air [2, 3].

A limiting factor for SPR sensitivity in these applications is the limited propagation length of SPPs due to a strong intrinsic damping of their EM field in metal. Even when the 'best plasmonic' metals, such as silver and gold, are used, the SPP propagation length is only about 10 μm in the optical frequency range. Other metals do not practically support any SPP propagation at visible frequencies. One way to increase the SPP propagation length and, consequently, the SPR sensitivity is to use long-range SPPs (LRSPPs), which can be achieved using a thin metal film embedded between two dielectrics with identical refractive indices (RIs) [4]–[7].

Moreover, as late as 1986, it was theoretically predicted [8] that the LRSPP propagation may be further increased if a slight asymmetry is added in the LRSPP structure, but experimental implementation of this slightly asymmetrical structure dielectric–metal–dielectric (D/M/D′) is rather complicated (see appendix A for details).

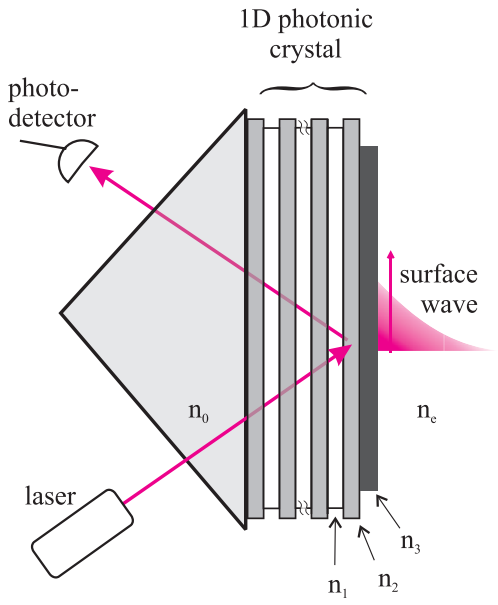

Figure 1. Excitation of optical SWs in a Kretschmann-like scheme.

In the work [9], another method for the excitation of LRSPPs was reported, in which the thin metal film was embedded between the medium being studied (with any RI, even a gas medium) and the 1D photonic crystal (1D PC). In such a structure (D/M/PC), a slight asymmetry in the EM field distribution may be introduced by a simple wavelength tuning.

Photonic crystals (PCs) are materials that possess a periodic modulation of their refraction indices on the scale of the wavelength of light [10]. Such materials can exhibit photonic band gaps that are very much like the electronic band gaps for electron waves traveling in the periodic potential of the crystal. In both cases, frequency intervals exist in which wave propagation is forbidden. This analogy may be extended [11] to include surface levels, which can exist in band gaps of electronic crystals. In PCs, they correspond to optical SWs with dispersion curves located inside the photonic band gap.

The one-dimensional photonic crystal (1D PC) is a simple periodic multi-layer stack. Optical surface modes in 1D PCs were studied in the 1970s, both theoretically [12] and experimentally [13]. Twenty years later, the excitation of optical SWs in a Kretschmann-like configuration was demonstrated [14]. A scheme of the Kretschmann-like excitation of PC SWs is presented in figure 1. In recent years, the PC SWs have been used in ever-widening applications in the field of optical sensors [15]–[20]. In contrast to SPPs, both p-polarized and s-polarized optical SWs (with a dielectric final layer of the 1D PC) [15, 17, 18] can be used in PC SW sensor applications. However, in applications in which the LRSPP propagates in a metal nanofilm deposited on an appropriate 1D PC surface (e.g. in hydrogen detection [19, 20]), only p-polarized waves can be used. Therefore, a unified theoretical description of PC SWs for both polarizations would be very useful, and such a description is presented in this paper. Additionally, the present paper describes conditions for the propagation of LRSPP in metal nanofilms (including lossy ones) that are deposited on the top of the 1D PC structure, and thereby provides the theoretical background for the works [9, 19, 20].

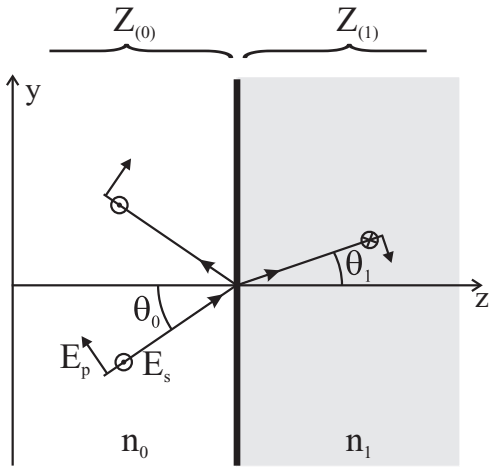

Figure 2. Reflection and transmission from a single interface.

2. Dispersion relation for s- and p-polarized surface waves in impedance terms

2.1. Impedance approach: basic definitions and the recursion relation for a multilayer

The 'characteristic impedance' of an optical medium is the ratio of the electric field amplitude to the magnetic field amplitude in this medium, i.e. $Z_{\text{char}} = E/H = 1/n$. The concept of impedance in the optics of homogeneous layers is based on a mathematical analogy between a cascade of transmission line sections and a multilayer optical coating.

For reflection from a plane interface, the useful value is the 'normal impedance' [21, 22] Z, which is the ratio of the tangential components of the electric field to the magnetic field:

$$Z = \frac{E_{\text{tan}}}{H_{\text{tan}}}. \tag{1}$$

Impedances for the s-polarized wave (in which the electric field vector is orthogonal to the incident plane—the TE wave) and for the p-polarized wave (in which the electric field vector is parallel to the incident plane—the TM wave) are correspondingly:

$$Z_{\text{s}} = \frac{E_x}{H_y} = \frac{1}{n\cos(\theta)} \quad \text{(for the TE wave)}, \tag{2}$$

$$Z_{\text{p}} = \frac{E_y}{H_x} = \frac{\cos(\theta)}{n} \quad \text{(for the TM wave)}. \tag{3}$$

For the interface between semi-infinite media 0 and 1 (figure 2), Fresnel's formula for reflection coefficients has a very simple form in impedance terms:

$$R = \frac{Z_{(1)} - Z_{(0)}}{Z_{(1)} + Z_{(0)}}, \tag{4}$$

where $Z_{(j)}$ is the normal impedance of medium j, given by (2) or (3). Hereafter, the use of R and Z (without subscripts s or p) means that the equation holds for both polarizations when the corresponding impedances Z_{s} or Z_{p} are inserted. Fresnel's formulae for transmission coefficients are as follows:

$$T_{\text{s}} = -2\frac{Z_{\text{s}(1)}}{Z_{\text{s}(1)} + Z_{\text{s}(0)}}, \tag{5}$$

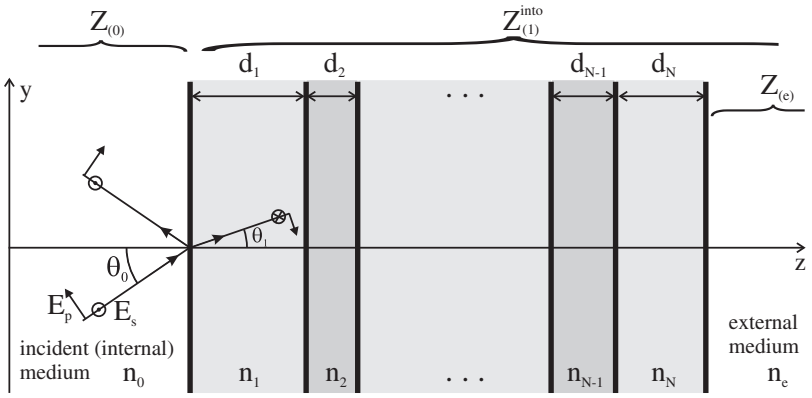

Figure 3. Reflection and transmission for a multilayer with N layers.

$$T_{\mathrm{p}} = -2\frac{n_0}{n_1}\frac{Z_{\mathrm{p}(0)}}{Z_{\mathrm{p}(1)} + Z_{\mathrm{p}(0)}}. \tag{6}$$

In figure 2, labeling the s-polarized wave in the first and second media by $\odot$ and $\otimes$ indicates the direction of the electric field vector $\vec{E}$ after transmission/reflection in accordance with our 'rule of signs'.

The equations for reflection coefficients of s- and p-polarized waves from any complex multilayer (see figure 3) also have a form similar to equation (4):

$$R = \frac{Z^{\mathrm{into}}_{(1)} - Z_{(0)}}{Z^{\mathrm{into}}_{(1)} + Z_{(0)}}, \tag{7}$$

where $Z^{\mathrm{into}}_{(1)}$ is an apparent input impedance for a multilayer, i.e. it is the impedance that is seen by an incoming wave as it approaches the interface.

If the multilayer is made up of N plane-parallel, homogeneous, isotropic dielectric layers (with RIs n_j and geometrical thicknesses d_j, where $j = 1, 2, \ldots, N$) between semi-infinite incident$_{(0)}$ and external$_{(e)}$ media (see figure 3), the apparent input impedance $Z^{\mathrm{into}}_{(j)}$ of a semi-infinite external medium$_{(e)}$ and layers from N to j may be calculated by the following recursion relation [21, 22]:

$$Z^{\mathrm{into}}_{(j)} = Z_{(j)}\frac{Z^{\mathrm{into}}_{(j+1)} - \mathrm{i}Z_{(j)}\tan(\alpha_j)}{Z_{(j)} - \mathrm{i}Z^{\mathrm{into}}_{(j+1)}\tan(\alpha_j)}, \tag{8}$$

where $\alpha_j = k_{z(j)}\,d_j = (2\pi/\lambda)n_j\cos(\theta_j)\,d_j$; $j = N, N-1, \ldots, 2, 1$ and $Z^{\mathrm{into}}_{(N+1)} = Z_{(N+1)} = Z_{(\mathrm{e})}$, $n_{N+1} = n_{\mathrm{e}}$ while $d_{N+1} = d_{\mathrm{e}} = 0$ by definition.

Fresnel's formulae for multilayer transmission coefficients are as follows:

$$T_{\mathrm{s}} = \prod_{j=0}^{j=N} T_{\mathrm{s}\left(\begin{smallmatrix} j+1 \\ j \end{smallmatrix}\right)}, \quad \text{with} \quad T_{\mathrm{s}\left(\begin{smallmatrix} j+1 \\ j \end{smallmatrix}\right)} = -\frac{\left(Z^{\mathrm{into}}_{\mathrm{s}\,(j+1)} + Z_{\mathrm{s}\,(j+1)}\right)}{\left(Z^{\mathrm{into}}_{\mathrm{s}\,(j+1)} + Z_{\mathrm{s}\,(j)}\right)}\,\mathrm{e}^{\mathrm{i}\alpha_{j+1}} \tag{9}$$

and

$$T_{\mathrm{p}} = \prod_{j=0}^{j=N} T_{\mathrm{p}\left(\begin{smallmatrix} j+1 \\ j \end{smallmatrix}\right)}, \quad \text{with} \quad T_{\mathrm{p}\left(\begin{smallmatrix} j+1 \\ j \end{smallmatrix}\right)} = -\frac{n_j Z_{\mathrm{p}\,(j)}}{n_{j+1} Z_{\mathrm{p}\,(j+1)}}\frac{\left(Z^{\mathrm{into}}_{\mathrm{p}\,(j+1)} + Z_{\mathrm{p}\,(j+1)}\right)}{\left(Z^{\mathrm{into}}_{\mathrm{p}\,(j+1)} + Z_{\mathrm{p}\,(j)}\right)}\,\mathrm{e}^{\mathrm{i}\alpha_{j+1}}, \tag{10}$$

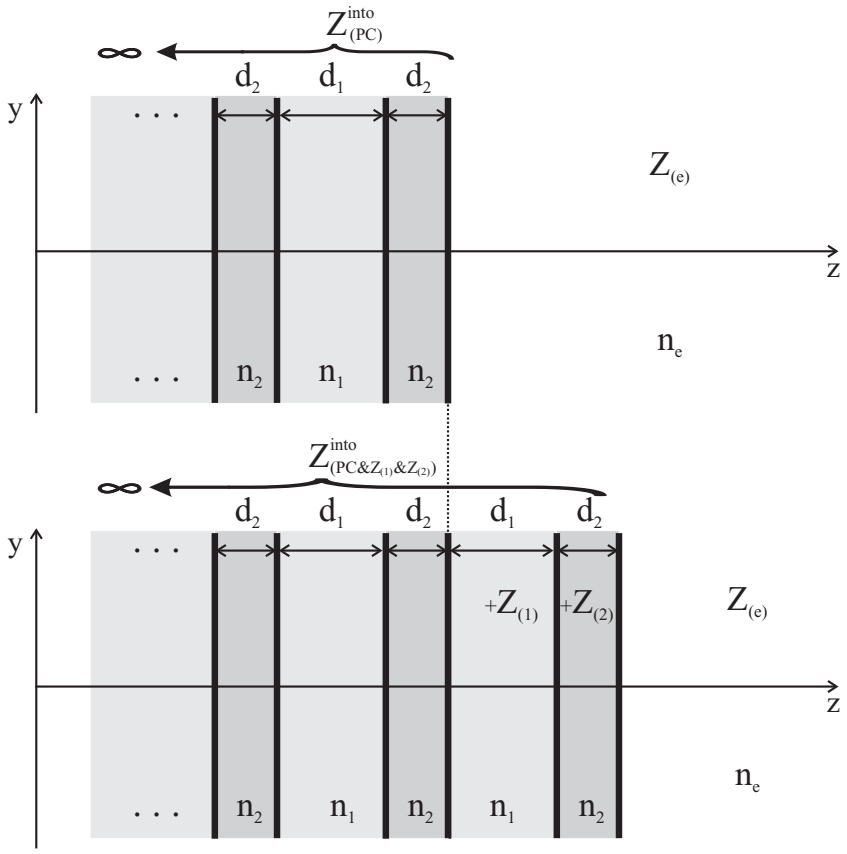

Figure 4. Determination of the impedance of the semi-infinite multilayer. Note that $Z^{into}_{(PC\&Z_{(1)}\&Z_{(2)})} \equiv Z^{into}_{(PC)}$.

where $T_{\binom{j+1}{j}}$ are the transmission coefficients at an interface between the jth layer and the $(j+1)$th layer.

2.2. The input impedance of a semi-infinite one-dimensional photonic crystal (1D PC)

Now, we are ready to obtain the input impedance of the 1D PC. Let us assume that we have a semi-infinite multilayer that consists of alternative layers with impedances $Z_{(2)}$ and $Z_{(1)}$ and its input impedance $Z^{into}_{(PC)}$ is unknown (see the top of figure 4). To find it, we play the next trick: first, we add an additional layer with impedance $Z_{(1)}$ to the multilayer and find the input impedance of this system using the recursion relation (8),

$$Z^{into}_{(PC\&Z_{(1)})} = Z_{(1)} \frac{Z^{into}_{(PC)} - iZ_{(1)} \tan(\alpha_1)}{Z_{(1)} - iZ^{into}_{(PC)} \tan(\alpha_1)}. \tag{11}$$

Then, we add an additional layer with impedance $Z_{(2)}$ to this system and obtain the same semi-infinite multilayer again (see the bottom of figure 4) with the input impedance:

$$Z^{into}_{(PC\&Z_{(1)}\&Z_{(2)})} = Z_{(2)} \frac{Z^{into}_{(PC\&Z_{(1)})} - iZ_{(2)} \tan(\alpha_2)}{Z_{(2)} - iZ^{into}_{(PC\&Z_{(1)})} \tan(\alpha_2)} \tag{12}$$

It is obvious that $Z^{\text{into}}_{(\text{PC}\&Z_{(1)}\&Z_{(2)})} \equiv Z^{\text{into}}_{(\text{PC})}$, and by solving equations (12) and (11) for $Z^{\text{into}}_{(\text{PC})}$, we obtain

$$Z^{\text{into}}_{(\text{PC})} = -\frac{\text{i}}{2}\frac{\left((Z^2_{(2)} - Z^2_{(1)})\tan(\alpha_2)\tan(\alpha_1) \pm \sqrt{s}\right)}{Z_{(2)}\tan(\alpha_1) + Z_{(1)}\tan(\alpha_2)}, \tag{13}$$

where

$$s = -4Z_{(1)}Z_{(2)}\left(Z_{(2)}\tan(\alpha_1) + Z_{(1)}\tan(\alpha_2)\right)\left(Z_{(1)}\tan(\alpha_1) + Z_{(2)}\tan(\alpha_2)\right) + \left[\left(Z^2_{(2)} - Z^2_{(1)}\right)\tan(\alpha_1)\tan(\alpha_2)\right]^2.$$

2.3. Dispersion relation for SWs

Now, we find the dispersion relation for SWs in 1D structures ended by an arbitrary layer with impedance $Z_{(3)}$. (It may be a layer with any n_3, for example a metal layer.) The input impedance of such a structure will be

$$Z^{\text{into}}_{(\text{PC}\&Z_{(3)})} = Z_{(3)}\frac{Z^{\text{into}}_{(\text{PC})} - \text{i}Z_{(3)}\tan(\alpha_3)}{Z_{(3)} - \text{i}Z^{\text{into}}_{(\text{PC})}\tan(\alpha_3)}. \tag{14}$$

A general condition for the existence of an SW between two media with impedances Z_{left} and Z_{right} is

$$Z_{\text{left}} + Z_{\text{right}} = 0. \tag{15}$$

In our case, this condition takes the form

$$Z^{\text{into}}_{(\text{PC}\&Z_{(3)})} + Z_{(\text{e})} = 0. \tag{16}$$

By solving equations (16) and (14), we obtain the dispersion relation for the optical SWs in the 1D PC:

$$\alpha_3 \equiv \left[k_{z(3)}d_3\right] = \pi M + \arctan\left(\frac{-\text{i}\left(Z^{\text{into}}_{(\text{PC})} + Z_{(\text{e})}\right)Z_{(3)}}{Z^2_{(3)} + Z^{\text{into}}_{(\text{PC})}Z_{(\text{e})}}\right), \tag{17}$$

where M is a whole number.

This is a general dispersion relation, which is valid for both polarizations. If one wishes to obtain the dispersion of the s-polarized optical SW, one should use the Z_{s} impedances in (17) and (13). Accordingly, to obtain the dispersion of the p-polarized optical SW, one must use Z_{p} impedances in (17) and (13).

It should be noted that the solution obtained for s-polarization is equivalent (at $M = 0$) to the solution derived from a dispersion relation for an s-polarized optical SW, which was deduced by Yeh *et al* [13] using the unit cell matrix method (see equation (58) in [12]). Meanwhile, the solution for p-polarization is equivalent to the solution derived from the dispersion relation for a p-polarized optical SW, which we deduced in a similar manner (using the unit cell matrix method) in [9] (see equation (2) in [9]). The dispersion relation (17) and the relations presented in [9, 12] were derived by different approaches (but, of course, both started from the same Maxwell equations and boundary conditions) and presented in different terms, but these relations give the same results and may be transformed to each other. The advantages of the presented dispersion relation with the impedance terms are its compact structure and its unified form for both polarizations. In addition, a visible physical interpretation of the impedance terms in the current dispersion relation allows it to be easily extended for use with more complicated

structures. For example, the addition of an adsorption layer between the layer$_{(3)}$ and the external medium$_{(e)}$ may be taken into account simply by changing the impedance $Z_{(e)}$ to the impedance $Z^{\text{into}}_{(e)}$ calculated via recursion relation (8), where the impedance of the external medium $Z_{(e)}$ is convoluted with the impedance of the adsorption layer $Z_{(a)}$.

2.4. Band gap maximum extinction per length

As a rule, in practical applications, we have the values of two RIs of alternative media in the 1D PC, and the aim is to find the thickness of each alternative layer, which provides the maximum extinction per length at given RIs, wavelength and angle. Below, we derive this condition for the maximum extinction, which makes it possible to minimize the overall thickness of the 1D PC. Also, we show that the commonly held opinion that it is a 'quarter-wavelength' thickness of the layers that provides the maximum extinction per length is incorrect.

To find the condition for the maximum extinction we derive the transmission coefficient for one period of the PC (two layers), that is, the transmission through the three interfaces,

$$T_{\left(\begin{smallmatrix}\text{PC}(j+3)\\ \text{PC}(j)\end{smallmatrix}\right)} = T_{\left(\begin{smallmatrix}\text{PC}(j+1)\\ \text{PC}(j)\end{smallmatrix}\right)} T_{\left(\begin{smallmatrix}\text{PC}(j+2)\\ \text{PC}(j+1)\end{smallmatrix}\right)} T_{\left(\begin{smallmatrix}\text{PC}(j+3)\\ \text{PC}(j+2)\end{smallmatrix}\right)}, \tag{18}$$

where expressions for $T_{\left(\begin{smallmatrix}j+1\\ j\end{smallmatrix}\right)}$ are given by equations (9) or (10). As a result we obtain for both polarizations

$$T_{\left(\begin{smallmatrix}\text{PC}(j+3)\\ \text{PC}(j)\end{smallmatrix}\right)} = \frac{\left(Z_{(2)} + Z^{\text{into}}_{(\text{PC})}\right)\left(Z_{(1)} + Z^{\text{into}}_{(\text{PC\&}Z_{(1)})}\right)}{\left(Z_{(1)} + Z^{\text{into}}_{(\text{PC})}\right)\left(Z_{(2)} + Z^{\text{into}}_{(\text{PC\&}Z_{(1)})}\right)} \mathrm{e}^{\mathrm{i}(\alpha_1+\alpha_2)}, \tag{19}$$

where $Z^{\text{into}}_{(\text{PC\&}Z_{(1)})}$ is given by (11) and $Z^{\text{into}}_{(\text{PC})}$ is given by (13).

The desired values of the thicknesses $d_1 = d_{1\max}$ and $d_2 = d_{2\max}$ are the thicknesses at which the next expression

$$f(d_1, d_2) = \left| \frac{\ln\left(\left| T_{\left(\begin{smallmatrix}\text{PC}(j+3)\\ \text{PC}(j)\end{smallmatrix}\right)} \right|\right)}{d_1 + d_2} \right| \tag{20}$$

reaches its maximum. Absolute values are inserted in equation (20) in order to obtain the same result regardless of the $\pm$ sign in equation (13). It may be noted that the 'quarter-wavelength' thicknesses of the layers, $d_j(\theta_j) = \lambda/(4n_j\cos(\theta_j))$, are values that maximize another expression, namely, expression (20) without the denominator, i.e. $(d_1 + d_2) \times f(d_1, d_2)$, and these 'quarter-wavelength' thicknesses are not optimal, especially at large incident (grazing) angles (i.e. at $\cos(\theta_j) \to 0$).

Now, we have all the equations required to calculate a 1D PC structure for any particular experimental conditions. Presented below is an example in which we obtain the 1D PC structure ending with a Pd nanolayer, which was successfully used for hydrogen detection in [19, 20].

3. Calculation of the 1D PC structure for particular experimental conditions

3.1. Angle-dependent variables

It will be very convenient to use a numerical aperture $\rho = n_0 \sin(\theta_0) = k_y(\lambda/2\pi)$ as an angle variable instead of angles θ_j in each jth layer and hereafter we will do so. It is a unified angle

variable for all layers, since according to Snell's law $\rho = n_0 \sin(\theta_0) = n_j \sin(\theta_j)$, for any j. The angle-dependent variables have the following forms as functions of ρ:

$$Z_{s(j)} = \frac{1}{n_j \cos(\theta_j)} = \frac{1}{n_j \sqrt{1-(\rho/n_j)^2}} \quad \text{(for the TE wave)}, \tag{21}$$

$$Z_{p(j)} = \frac{\cos(\theta_j)}{n_j} = \frac{\sqrt{1-(\rho/n_j)^2}}{n_j} \quad \text{(for the TM wave)}, \tag{22}$$

$$k_{z(j)} = \frac{2\pi}{\lambda} n_j \cos(\theta_j) = \frac{2\pi}{\lambda} n_j \sqrt{1-(\rho/n_j)^2} \quad \text{(for both polarizations)}. \tag{23}$$

3.2. Conditions for long-range propagation of the plasmon-polariton waves in metal films

The value of ρ at which we would like to excite a PC SW (and therefore a desired SW wavevector $k_{SW} = 2\pi\rho/\lambda$) depends on the particular problem that we are trying to solve. As an example, to excite LRSPPs in thin metal films, the effective RI of the LRSPPs ρ should be close to the RI of the external medium n_e. To prove this statement, in this subsection we will find the angular value ρ at which the electric field of the incident p-polarized wave has a minimum inside a thin layer with a *large extinction* for optical waves. This minimum coincides with the zero of the main, tangential component E_y of the electric field in the film with large extinction. This large extinction, i.e. large imaginary part of the RI of a thin film material ($\mathrm{Im}(n_M) \gg 1$), may arise both from a large negative permittivity of the material ($\mathrm{Re}(\varepsilon_M) \ll -1$, even at small $\mathrm{Im}(\varepsilon_M)$, as is the case for silver or gold) and from large losses in the material ($\mathrm{Im}(\varepsilon_M) \gg 1$, even at small or positive $\mathrm{Re}(\varepsilon_M)$, as is the case for palladium). In both cases the optical wave does not penetrate deeply into the bulk material with permittivity $\varepsilon_3 = \varepsilon_M$. It should also be noted that, in a very thin film, additional losses always appear due to collision-induced scattering of conducting electrons at the walls of the film. Therefore, the imaginary part of the permittivity in such a film is increased in comparison with the bulk material (see appendix B for details).

So, let us assume that we have a thin film with RI $n_3 = n_M$ and that a p-polarized light wave is incident on it with the angular parameter ρ. The instantaneous value of the tangential component of the electric field at a coordinate point z inside the film is the sum of the progressive and the recessive (reflected) waves,

$$\begin{aligned} E_y(z) &= E_{(+)} \, e^{-ik_{z(3)}(d_3 - z)} + E_{(-)} \, e^{ik_{z(3)}(d_3 - z)} \\ &= E_{(+)} \, e^{-ik_{z(3)}(d_3 - z)} + E_{(+)} R_{\left(\begin{smallmatrix} e \\ 3 \end{smallmatrix}\right)} \, e^{ik_{z(3)}(d_3 - z)}, \end{aligned} \tag{24}$$

where the reflection coefficient from the interface between the film$_{(3)}$ and the external medium$_{(e)}$ is given by (7):

$$R_{\left(\begin{smallmatrix} e \\ 3 \end{smallmatrix}\right)} = \frac{Z_{(e)} - Z_{(3)}}{Z_{(e)} + Z_{(3)}}. \tag{25}$$

To find the coordinate z_0 at which the tangential component of the electric field in the film is zero, we solve the equation

$$E_y(z_0) = 0 \tag{26}$$

with respect to z_0. Then we express the coordinate z_0 as $z_0 = d_3(1-\alpha)$, where α is the coordinate of the zero minimum z_0 in terms of film thickness d_3. When $z_0 = 0$ ($\rightarrow \alpha = 1$),

the zero of the E_y takes place at an internal border of the film. When $z_0 = d_3/2$ ($\rightarrow \alpha = 1/2$), the field zero occurs at the center of the film. When $z_0 = d_3$ ($\rightarrow \alpha = 0$), the field zero is located at an external border of the film. The solution of equations (26) and (24) is

$$\alpha \equiv [1 - (z_0/d_3)] = -\frac{\mathrm{i}\ln\left(-1/R_{\left(\begin{smallmatrix}\mathrm{e}\\3\end{smallmatrix}\right)}\right)}{2k_{z(3)}d_3}. \tag{27}$$

Assuming that $|n_3| \gg \rho \geqslant n_\mathrm{e}$, we will use the impedance of the final (metal) film in the so-called Leontovich approximation (see, for example, [23] for details). In this approximation, equations (22) and (23) have the form

$$Z_{\mathrm{p}(3)} = \frac{\sqrt{1-(\rho/n_3)^2}}{n_3} \approx \frac{1}{n_3}, \tag{28}$$

$$k_{z(3)} = \frac{2\pi}{\lambda} n_3 \sqrt{1-(\rho/n_3)^2} \approx \frac{2\pi}{\lambda} n_3, \tag{29}$$

while

$$Z_{\mathrm{p(e)}} = \frac{\sqrt{1-(\rho/n_\mathrm{e})^2}}{n_\mathrm{e}} \tag{30}$$

as usual.

Substituting (28), (29) and (30) into $R_{\left(\begin{smallmatrix}\mathrm{e}\\3\end{smallmatrix}\right)}$ of (25) and into equation (27) and then solving for ρ, we obtain (in the approximation $d_3 \ll \lambda$)

$$\rho_\alpha = n_\mathrm{e} + 2n_\mathrm{e}^3 \left[\alpha\pi \frac{d_3}{\lambda}\right]^2, \tag{31}$$

which we presented earlier (see equation (1) in [9]).

However, we have derived equation (31), which shows that the modulus of the electric field strength $|E_y|$ has a minimum equal to zero when the p-polarized EM wave is incident on the thin (metal) film in the angular range from ρ_1 to ρ_0. In this case, the point at which $|E_y| = 0$ is changed from the internal ($\alpha = 1$, $z_0 = 0$) to the external ($\alpha = 0$, $z_0 = 1$) borders of the film, and it is located at the center of the film at $\rho = \rho_{1/2}$ ($\alpha = 1/2$, $z_0 = 1/2$).

Now the next question arises: are there some EM surface modes with a wavevector in the range: $k = [\frac{\omega}{c}\rho_0 \cdots \frac{\omega}{c}\rho_1]$? If the answer is yes, one may expect that these modes will be long-range propagated surface modes, since they may be excited by the p-polarized waves incident on the film in the angular range $\rho = [\rho_0 \cdots \rho_1]$, and these modes have the zero minimum of $|E_y|$ inside the lossy (metal) film.

One example of such a mode is widely recognized—it is the LRSPP in a thin film embedded between two identical dielectrics. It is known that the dispersion curve of SPPs splits as a result of a coupling between SPPs from both film interfaces, and the LRSPP wavevector shifts (at a given frequency) to a light curve (i.e. $\rho \rightarrow n_\mathrm{e}$). The value of the LRSPP wavevector is $k \simeq \frac{\omega}{c}\rho_{1/2}$ (see [6] and/or appendix A), where $\rho_{1/2}$ is given by (31) at $\alpha = 1/2$, and the zero minimum of $|E_y|$ is always located at the center of the film.

PC SWs are another example of EM surface modes that can propagate along thin metal films and have a wavevector in the range of $k = [\frac{\omega}{c}\rho_0 \cdots \frac{\omega}{c}\rho_1]$. In the next subsection, we show how to design the PC structure for excitation of PC SW at desired $\rho \simeq [\rho_0 \ldots \rho_1]$ at given λ, n_1 and n_2.

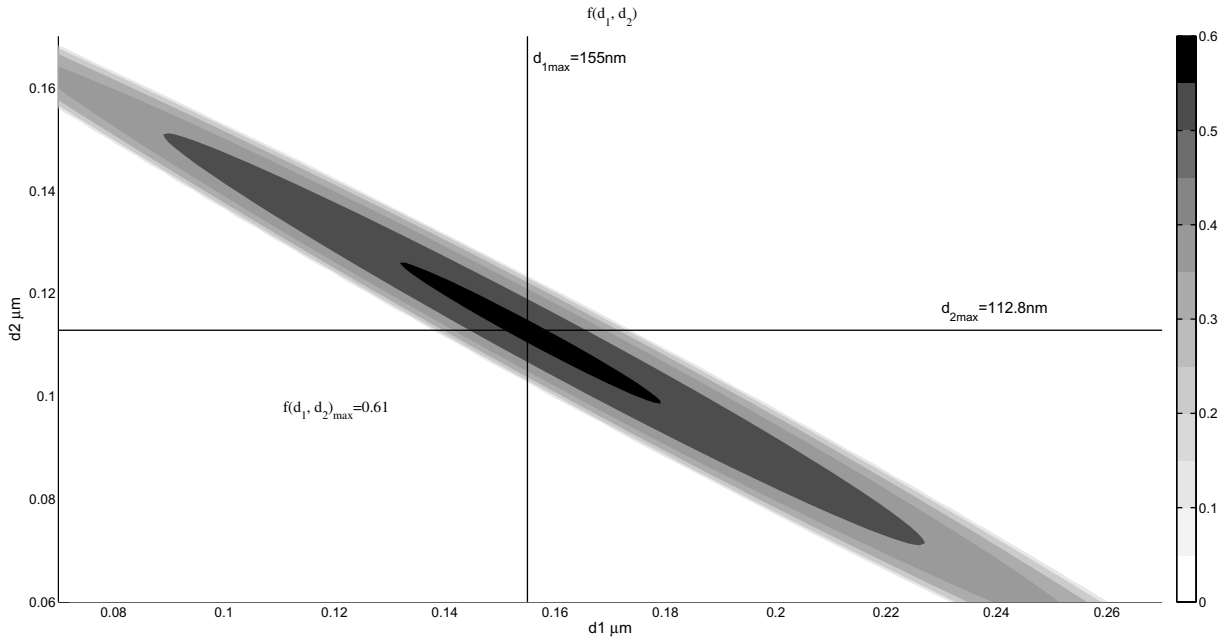

Figure 5. 1D PC band gap extinction as a function of layer thicknesses.

3.3. Derivation of d_1, d_2 and d_3 for the PC structure terminated by a Pd nanofilm

So, let us design the PC structure with maximum band gap extinction at desired $\rho \simeq \rho_{1/2} \simeq 1.0012$ (obtained from (31) at $n_e = 1.0003$, $d_3 \simeq 10\,\text{nm}$ and $\lambda \simeq 739\,\text{nm}$). Let us have two layer materials, Ta_2O_5 and SiO_2, with RIs of $n_2 = 2.076$ and $n_1 = 1.455$ at the wavelength of our tunable diode laser (at $\lambda \simeq 739\,\text{nm}$). The function $f(d_1, d_2)$ given by (20) is presented in figure 5. One can see that $f(d_1, d_2)$ reaches its maximum at $d_{1\max} = 155.0\,\text{nm}$ and $d_{2\max} = 112.8\,\text{nm}$. At these thicknesses, the maximum band gap extinction per length occurs and, therefore, the PC structure will have minimum overall thickness.

Now, we must find the thickness d_3 of the final palladium layer that will satisfy the dispersion relation (17). With $M = 0$ we have

$$d_3 = \frac{\lambda}{2\pi n_3 \sqrt{1-(\rho/n_3)^2}} \arctan\left(\frac{-\mathrm{i}\left(Z_{(\mathrm{PC})}^{\mathrm{into}} + Z_{(\mathrm{e})}\right) Z_{(3)}}{Z_{(3)}^2 + Z_{(\mathrm{PC})}^{\mathrm{into}} Z_{(\mathrm{e})}}\right). \tag{32}$$

Substituting $n_3 = n_{\mathrm{Pd}} = 1.9 + \mathrm{i}4.8$ and the other values pointed out in the present subsection into (32) (and into (22), (23) and (13) correspondingly), we obtain $d_3 = 1.2\,\text{nm}$. This is a rather small value and it is better for the thickness of the palladium layer to be in the range of 8–10 nm to be ensure that we will obtain a continuous film during deposition. If we want to retain the maximum band gap extinction at the desired $\rho_{1/2}$ and, therefore, do not want to change the optimal values $d_{1\max}$ and $d_{2\max}$, we may decrease the thickness of just the Ta_2O_5 layer, which is contiguous with the Pd layer. The decrease in thickness of the last Ta_2O_5 layer from $d_2 = 112.8\,\text{nm}$ to $d_2' = 103.4\,\text{nm}$ permits us to increase the thickness of the Pd layer to the value $d_3 = 8\,\text{nm}$ and satisfy the SW excitation condition at the desired angle $\rho_{1/2}$ and the desired wavelength λ.

Thus we derive the next PC structure: substrate/$(\mathrm{HL})^{14}\mathrm{H'M}$/air, in which H is a Ta_2O_5 layer with a thickness $d_2 = 112.8\,\text{nm}$, L is an SiO_2 layer with $d_1 = 155.0\,\text{nm}$, H′ is a Ta_2O_5 layer with $d_2' = 103.4\,\text{nm}$ and M is the palladium layer with $d_3 = d_{\mathrm{M}} = 8\,\text{nm}$. In figure 6, the

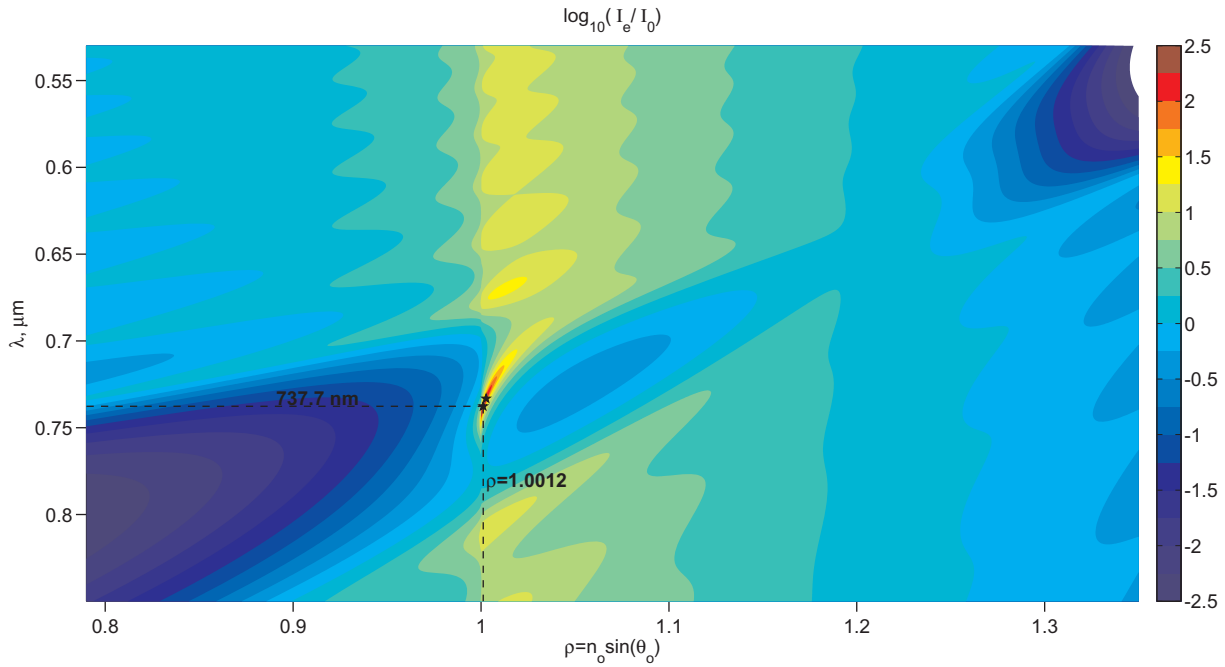

Figure 6. The calculated dispersion of the 1D PC structure with the terminal Pd nanolayer in air. The LRSPP mode is seen as the red curve (with an enhancement of more than 100) inside the band gap (blue areas with an enhancement of less than 1). The black pentagrams are experimental points measured at $\lambda = 737.7\,\text{nm}$ ($\rho = 1.0012$) and at $\lambda = 733.2\,\text{nm}$ ($\rho = 1.0027$). The photonic band gap vanishes near Brewster's angle ($\rho_{\text{Br}} \simeq 1.2$ in this system), where no reflection of the TM wave takes place from the SiO_2/Ta_2O_5 interface.

calculated dispersion of this 1D PC structure in air is presented as the logarithm of the optical field enhancement (i.e. as $\log T_{\left(\begin{smallmatrix}e\\0\end{smallmatrix}\right)}$) in the external medium near the structure. The optical field enhancement $T_{\left(\begin{smallmatrix}e\\0\end{smallmatrix}\right)}$ is calculated by using (10) and (8) for 29 dielectric layers and one metal nanolayer on BK-7 ($n_0 = 1.513$) substrate. The optimal number of Ta_2O_5/SiO_2 pairs depends on total extinction in the layers. In the present case, the Pd nanolayer is the layer that gives the main contribution in extinction and the 14 pairs provide the optimal coupling (i.e. $R_{\text{PC}} = 0$) of the incoming EM radiation into SWs.

The dispersion is presented using the coordinate $\lambda(\rho)$. The angular parameter ρ, at which the excitation of the surface mode occurs, is equal to the effective RI of the mode, n_{sw}. Therefore, the red curve that is inside the blue band gap in figure 6 presents the dispersion of the LRSPP mode (i.e. the dependence of its effective RI on the wavelength). The experimental points at $\lambda = 737.7\,\text{nm}$, $\rho = 1.0012$ and at $\lambda = 733.2\,\text{nm}$, $\rho = 1.0027$ are designated as black pentagrams and were excited by a tunable diode laser. One can see from figure 6 that in accordance with (31) the LRSPP mode exists near $\rho \sim n_{\text{e}}$ only ($\rho \simeq 1$–1.0026), where the minimum EM field inside the metal nanolayer occurs, while at $\rho > 1.0026$ the EM damping is increased significantly in this 8 nm thick metal film.

In the presented case, the optical surface mode dispersion curve approaches the line of the total internal reflection (TIR) ($\rho_{\text{TIR}} \equiv n_{\text{e}} = 1.0003$) at wavelengths in the range of $\lambda \sim$ 734–746 nm. Therefore, at these wavelengths, we can excite the SPP at $\rho \to n_{\text{e}}$ and expect it to

be LRSPP. At $\lambda = 733.7$ nm ($\rho = 1.0026 \simeq \rho_1$), the zero minimum of $|E_y|$ occurs at the internal interface of the 8 nm palladium film, while at $\lambda = 740.2$ nm ($\rho = 1.00088 \simeq \rho_{1/2}$) the zero minimum of $|E_y|$ occurs at the center of this 8 nm thick nanofilm. Moreover, at $\lambda = 745.6$ nm ($\rho = 1.000301$, i.e. $\rho \to \rho_0 \simeq n_e$) we can excite LRSPP with $|E_y| = 0$ near the external interface of the film, and this wave will have the largest propagation length. Theoretical propagation lengths, i.e. propagation lengths that take into account the internal damping in the Pd nanofilm but do not take into account the surface scattering of LRSPPs to photons, for these wavelengths are: $L_{733.7} = 0.14$ mm, $L_{740.2} = 0.32$ mm and $L_{745.6} = 5.4$ mm. Therefore, contrary to intuitive expectations, modes with $\rho = \rho_0 \to n_e$ ($|E_y| = 0$ at the external interface of the film, i.e. modes with an asymmetric field distribution in the nanofilm) are more long-range propagated than the mode with $\rho = \rho_{1/2}$ ($|E_y| = 0$ at the center of the film). More details about this issue are provided in appendix A.

4. Conclusions

The present paper provides the theoretical background and the algorithm for the design of 1D PC structures that support the propagation of optical SWs. We have used the impedance approach, which permits calculation for s- and p-polarizations by the same equations. The main results of this work are the input impedance of the semi-infinite 1D PC (13) and the dispersion relation of PC SWs (17). Equations (19) and (20) are needed for the design of a multilayer structure with maximal band gap extinction at the minimal overall thickness of the structure. Equation (31) is important for understanding the physical reasons for the propagation of the LRSPP even in thin films with large extinction, while the equations in appendix A provide additional insight concerning why slightly asymmetrical structures provide more long-range propagation of the SWs.

Acknowledgments

This work was supported financially by the Russian Federal Program 'Research and educational personnel for an innovative Russia', by the Russian Foundation for Fundamental Research and by the Science and Technology Cooperation Programme Switzerland–Russia. The author also thanks E V Alieva for useful discussions and assistance.

Appendix A. Dispersion relation for long-range surface plasmon polaritons (LRSPPs) in the symmetrical configuration and the increase of propagation length associated with slight asymmetry in the system

The propagation of LRSPP in a symmetrical structure (metal film between identical dielectrics) has been considered in several publications [3, 4, 6, 7]. Here, we will consider this point based on the impedance approach and then we will add slight asymmetry to the structure.

The dispersion relation, $\lambda(\rho)$, for SWs in a metal film between two semi-infinite dielectric media can be obtained easily, for example, from equation (17) or equation (32), in which the 1D PC is replaced by a uniform dielectric medium with an RI n_0 ($Z_{(PC)}^{into} \to Z_{(0)}$):

$$\frac{1}{\lambda} = \frac{1}{2\pi d_3 n_3 \sqrt{1-(\rho/n_3)^2}} \arctan\left(\frac{-i\left(Z_{(0)} + Z_{(e)}\right) Z_{(3)}}{Z_{(3)}^2 + Z_{(0)} Z_{(e)}}\right). \tag{A.1}$$

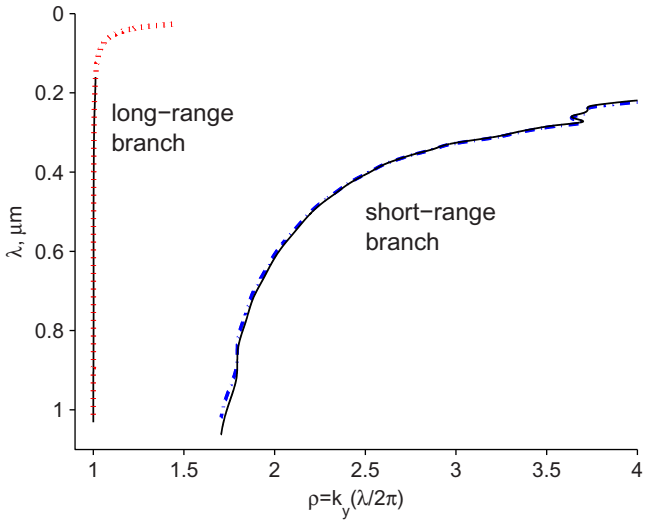

Figure A.1. The dispersion of a Pd nanofilm that is freely suspended in air. The solid black curve is calculated from the general dispersion relation for the symmetric system (A.2), whereas the dotted red curve and the dashed-dotted blue curve are calculated by approximated solutions (A.4) and (A.5), respectively.

For a pure symmetrical configuration ($n_0 = n_e$ and $Z_{(0)} = Z_{(e)}$), the general dispersion relation (A.1) has the form shown below:

$$\frac{1}{\lambda} = \frac{1}{2\pi d_3 n_3 \sqrt{1-(\rho/n_3)^2}} \arctan\left(\frac{-2iZ_{(e)}Z_{(3)}}{Z_{(3)}^2 + Z_{(e)}^2}\right). \tag{A.2}$$

By taking into account the Leontovich approximation, (28) and (29), the equation can be simplified further:

$$\frac{1}{\lambda} \simeq \frac{1}{2\pi d_3 n_3} \arctan\left(\frac{2\,n_3\,{n_e}^2\left(\rho^2 - {n_e}^2\right)^{-1/2}}{{n_e}^4 + {n_3}^2{n_e}^2 - {n_3}^2\rho^2}\right). \tag{A.3}$$

For a very thin film (at $d_3 \to 0$), one can obtain two solutions for ρ from (A.3):

$$\rho_{\mathrm{LRSPP}} \simeq n_e + \frac{n_e^3}{2}\left[\pi\frac{d_3}{\lambda}\right]^2, \tag{A.4}$$

$$\rho_{\mathrm{SRSPP}} \simeq \frac{\pi d_3 n_e^2}{3\lambda} - \frac{\lambda n_e^2}{\pi\,\mathrm{Re}(n_3^2)d_3} - \frac{\pi d_3\,\mathrm{Re}(n_3^2)}{2\lambda}. \tag{A.5}$$

The former equation presents an approximation for the long-range branch of the dispersion relation of a symmetrical system (A.2), while the latter is an approximation for the short-range branch (its damping increases at $d_3 \to 0$). In figure A.1, graphical illustrations of dispersion relation (A.2) (or (A.3), since no difference can be seen between them at this scale) and its approximations (A.4) and (A.5) are presented. Calculations are performed for an 8 nm thick Pd film that is suspended freely in the air ($n_e = 1.0003$), and the Pd RIs at different wavelengths were taken from [24]. In addition to good agreement between the dispersion equation for the symmetrical system and the approximated equations, figure A.1 shows that the long-range

branch of the curve has no noticeable wavelength dispersion in the visible range, while for the system with the PC from one side, the LRSPP curve (see figure 6) has prominent dispersion.

It is apparent that (A.4) coincides exactly with (31) at $\alpha = 1/2$, and therefore in a pure symmetrical configuration, the zero of the tangential component and the total minimum of the electric field are always located at the center of the metal nanofilm, which is not surprising due to the symmetry of the system. A more surprising fact is that this symmetrical system (with $|E_y| = 0$ at the center of the film) is not the optimal solution if one is looking for the smallest damping and the longest propagation length of the LRSPP. To the best of our knowledge, Wendler and Haupt were the first to point out this peculiarity. In the theoretical article [8], they showed, through numerical calculations, that, in a slightly asymmetrical structure, the propagation length may be three orders of magnitude greater than the propagation length in the symmetrical structure.

In experimental practice [9, 19], we have been able to increase the propagation length of SPPs by a factor in the range of 100–200 times. Further increase is limited by damping due to surface scattering, which occurs due to the close proximity of the effective RI of the LRSPP to the RI of the external medium or, in other words, 'the plasmon curve becomes too close to the light line'. Therefore, any small disturbance can transform plasmons to photons when ρ_{sw} is close to n_e. But, nevertheless, the internal damping of LRSPPs can be decreased when slight asymmetry exists in the structure.

Below, we obtain analytical expressions for the optimal Δn_{max} difference between the RIs of the dielectrics and show that the propagation length of the LRSPP increases when the minimum of the electric field shifts to the interface of the film (but does not leave the borders of the film). To do this, we return to the general dispersion relation for a non-symmetrical system (A.1) and assume that the RIs of the dielectrics on both sides of the metal film differ only by a small value Δn:

$$n_0 = n_e + \Delta n. \tag{A.6}$$

We are solving for the LRSPP wave only, so ρ will differ from n_0 by a small value $\Delta\rho$:

$$\rho = n_0 + \Delta\rho = n_e + \Delta n + \Delta\rho, \tag{A.7}$$

where $\Delta\rho \sim O(d_3^2/\lambda^2)$—see (A.4).

In the limit, with small $\Delta\rho$ and small Δn, the dispersion relation (A.1) can be simplified to the form

$$\lambda^{-1}(\Delta\rho, \Delta n) \approx \frac{1}{\pi d_3}\left(\frac{2}{n_e^9\,\Delta\rho}\right)^{1/2}\left[n_e^3\left(\Delta\rho + \frac{1}{4}\Delta n\right) - \left(\frac{1}{2}n_3^2 + \frac{9}{16}n_e^2\right)\Delta\rho\,\Delta n\right]. \tag{A.8}$$

Solving this equation for $\Delta\rho$ and taking its imaginary part, we obtain the next extinction of LRSPPs in a slightly asymmetrical system:

$$\begin{aligned}\mathrm{Im}\,[\rho_{LRSPP}(\Delta n)] &= \mathrm{Im}\,[n_0 + \Delta\rho] \\ &\approx \frac{\Delta n\,\mathrm{Im}(n_3^2)}{32 n_e^3 \lambda^2}\left(16\pi^2 d_3^2 n_e^3 + 3\pi^2 d_3^2 \Delta n\left(8\,\mathrm{Re}(n_3^2) + 9n_e^2\right) - 8\Delta n\lambda^2\right).\end{aligned} \tag{A.9}$$

This overapproximated imaginary part of the effective RI of the LRSPP has *two* solutions with (approximately) zero extinction ($\mathrm{Im}[\rho_{LRSPP}(\Delta n)] = 0$) and therefore with maximal propagation length: namely, the first solution is $\Delta n = 0$ (i.e. symmetric case) and the second solution is

$$\Delta n_{max} \approx 16\frac{\pi^2 d_3^2 n_e^3}{8\lambda^2 - 3\pi^2 d_3^2\left(8\mathrm{Re}(n_3^2) + 9n_e^2\right)}, \tag{A.10}$$

which in the limit $d_3 \approx 0$ is

$$\Delta n_{\max 0} \approx 2n_e^3 \left[\pi \frac{d_3}{\lambda}\right]^2. \tag{A.11}$$

One can see that (A.11) coincides with the addition to n_e from (31) at $\alpha = 1$ (i.e. when the minimum of the field is at the nanofilm border). Therefore, expression (A.10) may also be considered as a cutoff condition for the existence of LRSPPs (at $\Delta n > \Delta n_{\max}$, no bounded modes exist). From (A.1), it can be determined that, at $n_e = n_0 - \Delta n_{\max}$, the effective RI of LRSPP is close to the TIR angle, i.e. $\rho \simeq n_0$.

It is worth noting here that the analytical expression for $\Delta n_{\max}$ from (A.10) corresponds well with numerical data presented by Wendler and Haupt in [8]. Even the overapproximated expression for $\Delta n_{\max 0}$ from (A.11), which is not dependent on the nanofilm RI n_3, is coincident with these numerical data at small film thicknesses (i.e. at $d_3 \leqslant 15$ nm).

In excitation of ultra-long-range SPP in thin films by introducing a small asymmetry in the system, it is very important to maintain an appropriate balance between decreasing the internal damping of LRSPPs and increasing the scattering of the LRSPPs. The possibility for tuning system parameters during the experiment to find the optimum is extremely convenient in this case.

The principal difference between $D/M/D'$ and $D/M/PC$ systems is that, in the system with a 1D PC on one side, it is experimentally easy to introduce such a small asymmetry (in effective RI) by tuning the wavelength of the laser, while it is really difficult to (finely) tune the dielectric constants on one interface by any means. Wavelength tuning would not be useful in the $D/M/D'$ case, because dispersion of dielectrics is small in non-absorbing wavelength regions, while wavelength tuning in the PC structure is very effective due to the high-wavelength dispersion inside the band gap regions.

In concluding this subsection, it is worth noting that such a slight asymmetry can also be introduced by a thin dielectric film near one side of the metal nanofilm. For example, this dielectric film may be a membrane, supporting the metal nanofilm in a gaseous (or liquid) environment [25]. Using the same impedance approach, in a zeroth-order approximation, it is easy to show that the optimal thickness of the dielectric film (membrane) with RI n_a should be near or less than $d_{\max 0}$, i.e.

$$d_a \leqslant d_{\max 0} \approx \frac{d_3 n_a^2}{n_a^2 - n_e^2}. \tag{A.12}$$

If the thickness of the dielectric film is more than $d_{\max 0}$, then internal damping of LRSPPs in such a system considerably increases.

Appendix B. Additional damping in a thin film

Damping of EM waves in thin metal films increases due to collision-induced scattering of conducting electrons at the walls of the film. This occurs when the mean free path of the electrons becomes comparable to the characteristic dimensions of the system. Therefore, the imaginary part of the permittivity in such a film is increased in comparison with the bulk material. Unfortunately, in many articles (especially theoretical articles), authors have usually disregarded this fact and used overly optimistic values for the imaginary part of the metal permittivity of nanofilms.

Here we present a summary of formulae for this case, which help us to estimate the minimal addition to $\mathrm{Im}(\varepsilon_M) \equiv \varepsilon''_{bulk}$. At optical frequencies, the damping in nanostructures with the characteristic dimension L is

$$\gamma = \gamma_{bulk} + \frac{v_F}{L}, \tag{B.1}$$

where γ_{bulk} is the damping constant for the bulk sample and v_F is the electron velocity on the Fermi surface. Below, several specific cases are considered.

B.1. Nanofilm as a set of nanoparticles

For a sphere [26]

$$\varepsilon'' = \frac{\omega_p^2}{\omega^3}\gamma = \frac{\omega_p^2}{\omega^3}\left(\gamma_{bulk} + \frac{3v_F}{4r}\right) = \varepsilon''_{bulk} + \frac{3}{4}\frac{\omega_p^2}{\omega^3}\frac{v_F}{r}, \tag{B.2}$$

where ω_p is the plasma frequency. Therefore, the characteristic dimension in this case is $L = L_r = 4r/3$ (r is the radius of the sphere).

B.2. Continuous film

For a continuous film with thickness d [27],

$$\gamma = \gamma_{bulk} + \frac{3\omega_p}{8}\frac{v_F}{c}\frac{1+\cosh^2(\omega_p d/c)}{\sinh(\omega_p d/c)\cosh(\omega_p d/c) + \omega_p d/c}. \tag{B.3}$$

For a very thin film (nanofilm), in the limit $d \to 0$

$$\gamma = \gamma_{bulk} + \frac{3}{8}\frac{v_F}{d} \tag{B.4}$$

(therefore $L = L_d = 8d/3$ in this limit) and

$$\varepsilon'' = \frac{\omega_p^2}{\omega^3}\left(\gamma_{bulk} + \frac{3v_F}{8d}\right) = \varepsilon''_{bulk} + \frac{3}{8}\frac{\omega_p^2}{\omega^3}\frac{v_F}{d}, \tag{B.5}$$

while in the general case

$$\varepsilon'' = \varepsilon''_{bulk} + \frac{3\omega_p^3}{8\omega^3}\frac{v_F}{c}\frac{1+\cosh^2(\omega_p d/c)}{\sinh(\omega_p d/c)\cosh(\omega_p d/c) + \omega_p d/c}. \tag{B.6}$$

We have considered only collision-induced damping, and we did not take into account other types of damping in small volumes, which may lead to further increases of the imaginary part of the nanosized materials at optical frequencies.

The collision-induced damping increase in the nanofilm at zero frequency may be estimated by Fuchs' formula [28] for a specific electrical resistance of continuous films. For example, in our work with a gold nanofilm [9], the electrical resistance of the nanofilm was 850 Ω for a strip that was 0.25 mm wide and 6.5 mm long. Therefore, for our nanofilm thickness of 5 nm, the specific resistance in the nanofilm was $\rho_{film} = 16.3\ \mu\Omega\,\mathrm{cm}$, which is 7.4 times greater than the specific resistance of bulk gold ($2.2\ \mu\Omega\,\mathrm{cm}$). According to Fuchs' formula at $d \ll l_0$ [28]

$$\frac{\rho_{bulk}}{\rho_{film}} = \frac{3d}{4l_0}\ln\left(\frac{l_0}{d}\right). \tag{B.7}$$

Substituting the mean free path of electrons in bulk gold, which at room temperature is $l_0 \simeq 50$ nm, we obtain that the specific resistance of the 5 nm gold film at room temperature should be about 6 times greater than that of bulk gold. This value is in good agreement with the measured value, taking into account imperfections of the sputtered gold nanofilm.

References

[1] Raether H 1988 *Surface Plasmons* (Berlin: Springer)
[2] Liedberg B, Nylander C and Lundström I 1983 *Sensors Actuators* **4** 299–304
[3] Berini P 2008 *New J. Phys.* **10** 105010
[4] Sarid D 1981 *Phys. Rev. Lett.* **47** 1927–30
[5] Craig A E, Olson G A and Sarid D 1983 *Opt. Lett.* **8** 380–2
[6] Yang F, Sambles J R and Bradberry G W 1991 *Phys. Rev.* B **44** 5855–72
[7] Berini P 2009 *Adv. Opt. Photon.* **1** 484–588
[8] Wendler L and Haupt R 1986 *J. Appl. Phys.* **59** 3289–90
[9] Konopsky V N and Alieva E V 2006 *Phys. Rev. Lett.* **97** 253904
[10] Yablonovitch E 1993 *J. Opt. Soc. Am.* B **10** 283–95
[11] Kossel D 1966 *J. Opt. Soc. Am.* **56** 1434
[12] Yeh P, Yariv A and Hong C S 1977 *J. Opt. Soc. Am.* **67** 423–38
[13] Yeh P, Yariv A and Cho A Y 1978 *Appl. Phys. Lett.* **32** 104–5
[14] Robertson W M and May M S 1999 *Appl. Phys. Lett.* **74** 1800–2
[15] Konopsky V N and Alieva E V 2007 *Anal. Chem.* **79** 4729–35
[16] Shinn A and Robertson W 2005 *Sensors Actuators* B **105** 360–4
[17] Konopsky V N and Alieva E V 2009 Optical biosensors based on photonic crystal surface waves *Biosensors and Biodetection, Methods and Protocols, Volume 1: Optical-Based Detectors (Springer Protocols: Methods in Molecular Biology* vol 503) ed A Rasooly and K E Herold (Totowa, NJ: Humana Press) chapter 4 pp 49–64
[18] Konopsky V N and Alieva E V 2010 *Biosens. Bioelectron.* **25** 1212–6
[19] Konopsky V N and Alieva E V 2009 *Opt. Lett.* **34** 479–81
[20] Konopsky V N, Basmanov D V, Alieva E V, Dolgy D I, Olshansky E D, Sekatskii S K and Dietler G 2009 *New J. Phys.* **11** 063049
[21] Brekhovskikh L 1980 *Waves in Layered Media* (New York: Academic)
[22] Delano E and Pegis R 1969 Methods of synthesis for dielectric multilayer filters *Progress in Optics* vol VII ed E Wolf (Amsterdam: North-Holland) chapter 2 pp 67–137 (see pp 77, 130)
[23] Senior T 1960 *Appl. Sci. Res.* B **8** 418–36
[24] Palik E D 1985 *Handbook of Optical Constants of Solids* (London: Academic)
[25] Berini P, Charbonneau R and Lahoud N 2007 *Nano Lett.* **7** 1376–80
[26] Bohren C and Huffman D 1983 *Absorption and Scattering of Light by Small Particles* (New York: Wiley)
[27] Thèye M 1970 *Phys. Rev.* B **2** 3060–78
[28] Larson D C 1971 Size-dependent electrical conduction in thin metal films and wires *Physics of Thin Films* vol VI ed M H Francombe and R W Hoffman (London: Academic) chapter 2 pp 81–149